Nuclear Inst. and Methods in Physics Research B 478 (2020) 50–55

Contents lists available at ScienceDirect

Nuclear Inst. and Methods in Physics Research B

journal homepage: www.elsevier.com/locate/nimb

Millimeter wave photoresponse of low-dose radiation damaged silicon

Biswadev Roy[a,*], Branko Pivac[b], Branislav Vlahovic[a], Marvin H. Wu[a]

[a] Department of Mathematics & Physics, North Carolina Central University, Durham, NC 27707, USA
[b] Ruđer Bošković Institute, Bijenička cesta 54, 10000 Zagreb, Croatia

ARTICLE INFO

Keywords:
Time-resolved
Millimeter
Transmission
Reflection
Irradiation
Fluence
Radiation

ABSTRACT

This paper is about analyzing millimeter wave probe signal (150 GHz) differential absorption datasets to reveal some changed transmission and reflection properties of 500 µm p-doped Si wafers exposed to 1.2, 2.0, and 0.75 MeV gamma, proton, and chlorine ion beams (with doses in range 0.1 to 6 MGy). The decay portion of the respective pristine and irradiated sample RF responses were tri-exponentially fitted, and respective time constants evaluated as function of radiation dose. The peak RF voltages and their ratio with the transmitted DC voltages at each of the 532 nm laser radiation fluence points were plotted as function of laser radiation itself. Radiation dose is found to enhance the third time constant τ_3 that decays very fast beyond 0.1 MGy. Average τ for all irradiated samples correlates negatively with radiation dose (R = −0.83). 4-probe resistivity of 2 MeV H^+ exposed samples increase ~10x and enhances the peak RF voltage to DC voltage ratio ($\Delta V_T/V_{dc}$). Chlorine (Cl^{2+}) irradiated Si wafers show feeble $\Delta V_T/V_{dc}$ compared to those exposed with γ or H^+ beam. DC transmittances of all samples at 150 GHz lie in the range 0.46–0.64.

1. Introduction

Radiation damage due to proton and photon irradiation in opto-electronic semiconductors and its effect in photoconductivity have been well reported previously [1–10]. Point defects and cluster defects in silicon develop due to non-ionizing energy loss of radiation. The latest research on the fusion and space exploration calls for further research in this direction [11,12]. Constant exposure to low dose gamma radiation due to presence of radiation sources in the vicinity have caused reduction in performance of solar PV modules and increase in photocurrent and power while photovoltage is constant [13]. General forms of radiation effects observed on materials are impurity production, atomic displacements, removal of electrons from atoms (ionization) and large energy release in a very confined volume resulting in thermal heating. High energy proton can significantly damage the crystal lattice resulting in exhibition of high resistivity of the samples [2]. Kishimoto et al., 1996 [8] have well documented the radiation damage of Si for its exposure to electron, neutron, proton, various other ions and gamma. Amekura et al., 1998 [5] have pointed out that while developing radiation resistant electronic devices involving Si it is very important to reveal elementary processes in semiconductors. Effects of irradiation with beams with around 17 MeV proton on Si were well studied and reported for Si [3,5,14], another set of results are published for studies on structural defects induced in Si at GeV energy levels [6,15,16]. Transient conductivity changes in pulse radiolysis technique were studied for Si on glass, and CdS (Fluka) powder using the time-resolved microwave conductivity apparatus Warman et al., 1989 [4]. They used a pump-probe apparatus delivering 3 MeV electron beam from a Van de Graaf generator as pump beam on sample, and 100–200 mW 26.5 GHz to 38 GHz (sweeping mode) microwave signal used as probe beam. In this work they had presented the microwave absorption peak voltages normalized by the beam charge in nC as function of time for different dose level ranging from 1.2 Gy to 47.5 Gy. In their experiments, the samples were contained in a microwave cell and waveguide was used for transport of the probe signal to sample and the detector system.

Relevant to these studies attempted earlier, our experiment design was for noting the transient conductivity changes at 150 GHz due to carrier generation in irradiated Si samples when pumped by laser with ~0.7 µJ cm^{-2} radiation fluence at 532 nm wavelength. We used a Time-Resolved millimeter Wave Conductivity apparatus (TR-mmWC) [17] for data acquisition. Data were collected at fixed probe frequency but we swept the pump laser radiation fluence levels between 0.1 and 10 µJ cm^{-2}. We then perform initial tri-exponential fitting of the averaged voltage time traces, and calculate time constants for and attempt to study differences of these time constants from those obtained for the pure Si sample values.

Ion-induced damages in semiconductor are well simulated using standard Monte Carlo based Stopping and Range of Ions in Matter

* Corresponding author.
E-mail address: broy@nccu.edu (B. Roy).

https://doi.org/10.1016/j.nimb.2020.05.012
Received 3 March 2020; Received in revised form 7 May 2020; Accepted 8 May 2020

Table 1
List of samples and property. Sample 1 is boron doped P type c-Si wafer and rest (2 through 8) are irradiated versions of the same wafer. Resistivities were measured using 4-probe system and dc transmissions were measured using TR-mmWC operated at 150 GHz CW, with beam power in the vicinity of 0.32 mW. ^{60}Co doses in MGy were measured while sample was irradiated, H^+ and Cl^{2+} doses shown in italics (column 4) were computed using the SR-NIEL calculator v6.0.1 (June 26, 2019).

Sample	Resistivity (Ohm-cm)	DC transmission (%)	Exposure*	SRIM Total Vacancy
1	15.13 ± 0.375	64.15	Pristine	
2	15.47 ± 0.24	57.8	0.1 MGy γ 1.2 MeV	285/Ion
3	15.43 ± 0.41	57.5	0.5 MGy γ 1.2 MeV	
4	15.84 ± 0.32	60.1	1.0 MGy γ 1.2 MeV	
5	150.01 ± 14.59	53.7	10^{12} H^+/cm^2 2 MeV *5.3 Gy*	36/Ion
6	54.5 ± 3.5	50.9	10^{14} H^+/cm^2 2 MeV *0.00531 MGy*	
7	15 ± 1.46	46.9	10^{12} Cl^{2+}/cm^2 0.75 MeV *5.97 MGy*	4168/Ion
8	15.68 ± 0.05	50.3	10^{14} Cl^{2+}/cm^2 0.75 MeV *5.97 MGy*	

(SRIM) model [18] which is used to calculate the total vacancy introduced per ion in each of the irradiated sample. Gamma dosages were measured during irradiation process itself but dosages for proton and chlorine ions were computed using the Screened Relativistic Non-Ionizing Electron Loss (SR-NIEL) calculator [19].

The contactless TR-mmWC system used for this work is operated in free space configuration and uses a quasi-optical setup. The system has previously been calibrated using 550 µm c-Si samples with resistivities in the range 16–120 Ω-cm. The detector system has two outputs (RF and dc) and the ratio can be related to the finite photoconductance change ΔG,

$$|\Delta V_{RF}/V_{dc}| = -K\Delta G \tag{1}$$

K is the sensitivity factor and was evaluated as 0.2 in previous studies using Si data [17]. Intrinsic resistivities of each exposed sample were measured using the standard 4-probe technique and we note that they are changed due to vacancies imparted by energetic photons and ions. In Table 1 we present Si properties evaluated after irradiation and some computed from standard models.

Overall, in this paper we perform an initial data analysis (IDA) of the radiofrequency (RF) transients that are captured by the detector in voltage form to i) show the nature of average transients taken for various irradiated samples in transmission mode and reflection mode and explain the data acquisition strategy in brief. ii) perform IDA of the stored transmitted voltage transients by tri-exponential fitting of the decay portion of each trace and study the difference of the 3 time constants and the average time constant so computed for different samples after fitting to exploratively understand its relationship with the doses of radiation, vacancies introduced, and its relation with measured 4-probe resistivity of each sample. These results are given in section 2.1. iii) Photo-absorption induced ΔV_{RF} peak in transmitted transients obtained using 500 µm thick Si samples irradiated by 1.2 MeV gamma radiation, 2 MeV H^+ (proton) and 0.75 MeV Cl^{2+} ion at various fluences are analyzed in terms of laser radiation fluence. These results are shown in section 2.2.

2. Time-resolved response of irradiated silicon samples

The quasi-optical setup of TR-mmWC is well explained in ref. 17. The advantage of millimeter wave probing of irradiated silicon is that it enables us to acquire non-resonant absorption profile occurring in irradiated specimens that have dimensions comparable to that of the probe wavelength. This results in acquisition of millimeter wave (mmw) data for states between surface impedance in the reflection profile and accounting the depolarization factors resulting in transmission profile. Boron-doped Czochralski-grown single-crystal silicon sample used for this experiment has (1 0 0) orientation, intrinsic resistivity15.13 ± 0.375 O-cm and 500 µm thickness. Additional Si wafers of exact quality as the pristine sample wafer were irradiated with 1.2 MeV γ radiation from a ^{60}Co source, at doses 0.1 MGy (exposure for 19.9 Ks), 0.5 MGy (exposure for 59.4 Ks), and 1 MGy (exposure for 119Ks). These were achieved at room temperature. When the samples were inserted into the ^{60}Co source for γ irradiation its temperature rise were recorded in the range 20–40 °C. Proton beam with energy level 2 MeV was used on similar Si wafer having same dimensions as the pristine (sample 1 in Table 1) at particle fluence of 10^{12} H^+/cm^2 and 10^{14} H^+ cm^{-2} respectively obtained from a 6 MV Van de Graaf accelerator at Boskovic Institute, Zagreb. Chlorine (Cl^{2+}) ions at energy 0.75 MeV and fluences 10^{12} Cl^{2+} cm^{-2} and 10^{14} Cl^{2+} cm^{-2} were also used for irradiating similar Si wafer at room temperature using the same Van de Graaff accelerator.

Table 1 lists the resistivity, 150 GHz transmittance, exposure type, dose and total vacancies (per-ion) of the irradiated Si samples. Transmission and reflection voltages are captured using an antenna fed 110–170 GHz input zero bias Schottky diode detector (ZBD) [20] with a bias-tee, gain 31.48 dB and RF output in the range 0.1–6000 MHz. This ZBD is a negative voltage detector.

Fig. 1(a) and (b) above show the peak and decay of the transmitted and reflected RF voltages captured for each irradiated sample shown as function to delay time (s). The traces shown in Fig. 1 are obtained after averaging the signal 5 k to 40 k times. Chlorine ion induced defects are found to impede the TR-mmWC peak voltage response very sharply. Chlorine being a heavy ion introduces rapid change in Si wafer optical property thereby making it less transparent to the probe beam even after being excited by the pump at the maximum laser radiation fluence level.

2.1. Decay response of irradiated Si data

The low noise probe beam transmission and reflection traces shown in Fig. 1 are obtained after the beam electric field has interacted with the effective electric field of the electron-hole pairs when the pump-probe focused spot (with $1/e^2$ pump-probe beam diameter ratio ~3.6) is excited by the 532 nm laser at a maximum power of 22.14 mW (maximum laser radiation fluence ~10 µJ cm^{-2}) with spot size ~10 mm^2.

A complete carrier decay in semiconductor is well represented by the following non-radiative process combination:

$$\frac{-dn}{dt} = K_1 n + K_2 n^2 + K_3 n^3 \tag{2}$$

where n is the carrier concentration number/cm^3, K_1, K_2, and K_3 represent the coefficients of the rate equation representing the defect induced (Shockley-Read-Hall) trap-assisted process, the non-radiative

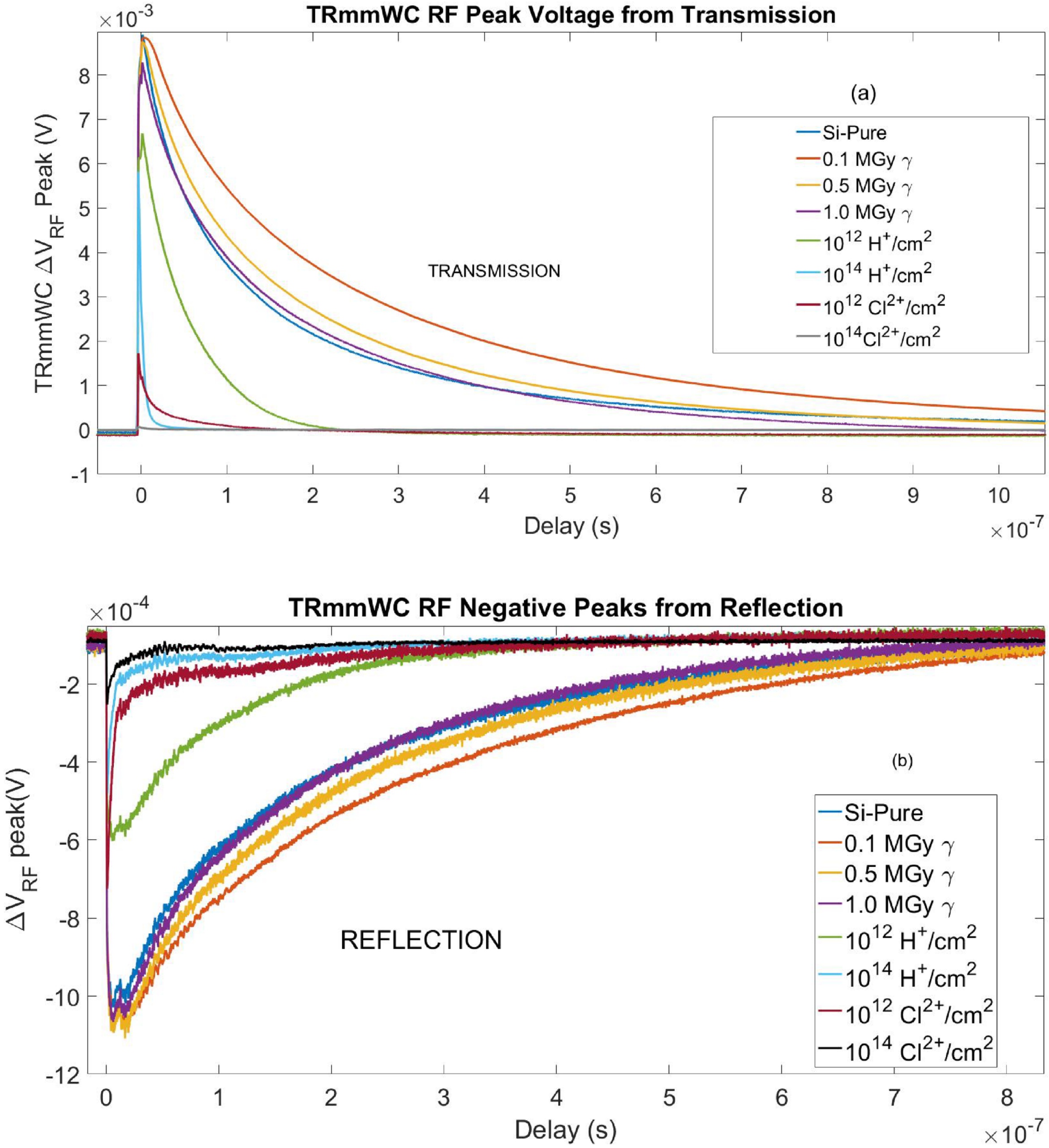

Fig. 1. (a) Delay time traces of 150 GHz probe voltage signal transmitted, and (b) reflected and captured by antenna fed ZBD (negative voltage detector) when pristine and irradiated Si samples are activated by 532 nm pump photon fluence ~10 μJ cm^{-2}. Note: diminished Cl^{2+} irradiated response.

band-to-band, and the heavily doped/high injection level Auger recombination (3 carrier interaction) constants. In light of Eq. (2) and the TR-mmWC data that we collected it needs to be pointed out that the 532 nm laser radiation fluence was maintained at 0.7 μJ cm^{-2} and at that moderate level of fluence, with the given beam spot-size and the pump repetition rate of 1 kHz with a pulse-width ~0.7 ns the carrier densities are ~9×10^{15}cm^{-3} after assuming 100% quantum efficiency. The dopant concentration (n_0) for the 15.5 Ω-cm resistivity Si wafer is calculated from PV Lighthouse (PVL) calculator [21] to be 8.71×10^{14} cm^{-3}. The net carrier density (Δn) ~8.1×10^{15} cm^{-3}. Looking up the ambipolar Auger coefficient data computed by Eq. (22) in Kerr and Cuevas, 2002 [22] we note that for our Δn the coefficient is 0.5×10^{-29} cm^6 s^{-1}, Auger lifetime ~100 ms, and Auger recombination enhancement factor is around 10. Based on PVL resources it is seen that SRH trap assisted process lifetimes are 1/1280 of the typical Auger lifetimes for Si.

However, when viewing the decay portion of the signals so obtained for each of the irradiated samples, it is found that not one exponential decay will perfectly be able to reconstruct the decay signal. Residuals in such a model remained very high. Hence, we approached IDA path and obtained a tri-exponential fitting as the best model to show minimum residual with the experimental data of the RF voltage transients.

$$V_{RF} = a\exp(-t/\tau_1) + b\exp(-t/\tau_3) + c\exp(-t/\tau_3) \tag{3}$$

Average τ is computed after obtaining the Eq. (3) parameters from the experimental data.

$$\tau_{avg} = \frac{a\tau_1 + b\tau_2 + c\tau_3}{(a + b + c)} \tag{4}$$

V_{RF} is the differential signal voltage acquired by detector that results from the probe light absorption by carrier population (Δn) created due to pump action. The pulse peaks and then decays fast as shown in Fig. 1.

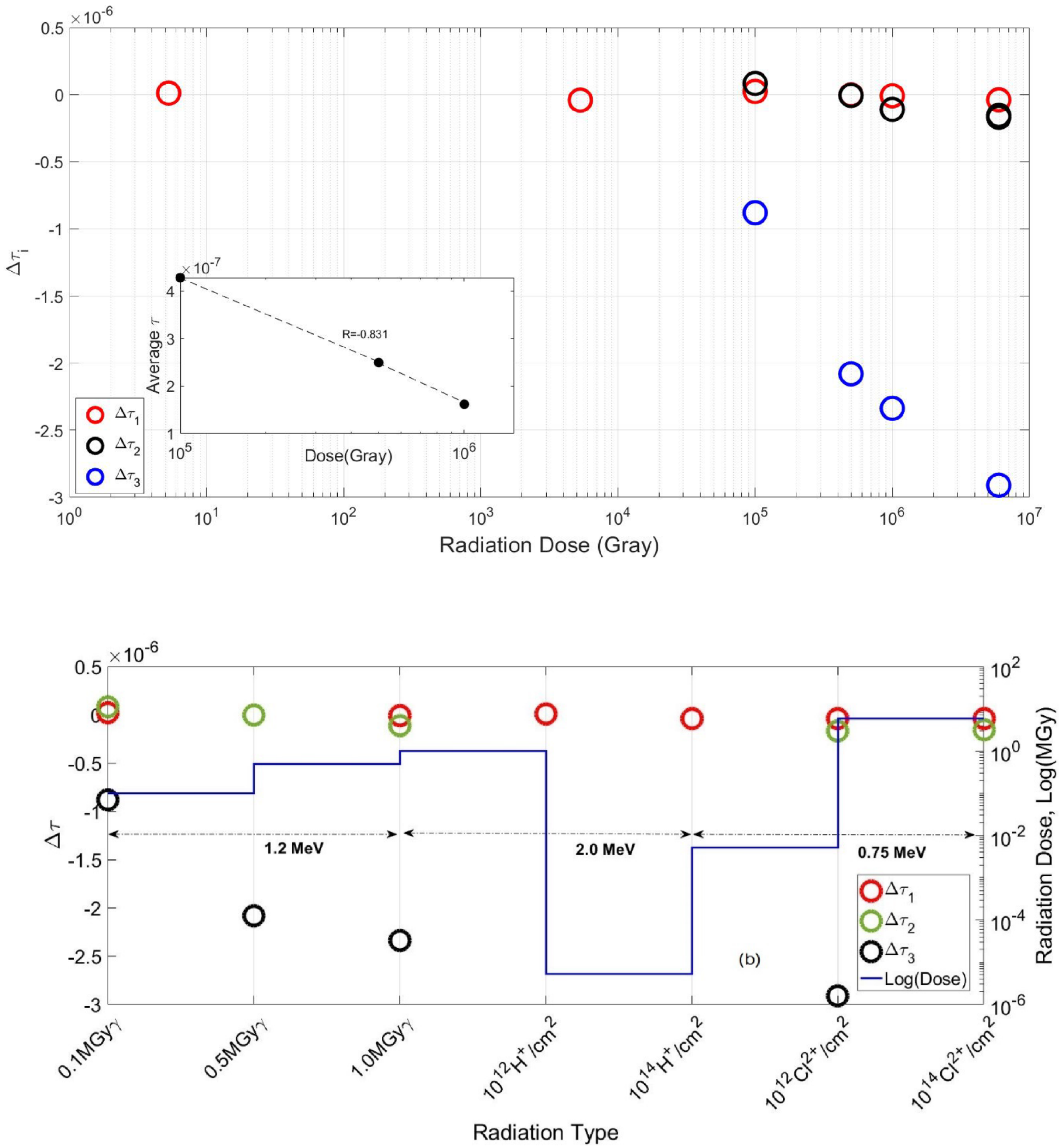

Fig. 2. (a) Change in calculated decay time of the RF responses $\Delta\tau_1$, $\Delta\tau_2$, and $\Delta\tau_3$ arising from transmitting 150 GHz probe signal through irradiated Si wafers when excited by a 0.7 ns width 532 nm laser with fluence ~0.7 μJ cm^{-2}. The Δτ's are computed with respect to the pristine c-Si (Δτ irradiated sample minus Δτ pristine Si) shown as function of radiation dose; inset of Fig. 2a: shows variation of available average τ calculated using Eq. (4) with respect to the radiation dose with an appreciable negative correlation R = −0.831, (b) variation of the differences in same lifetime shown in Fig. 2a but in terms of the exposure type with the logarithm of respective dosages shown in solid blue line and labeled y2 ordinate; beam energy level for each type of radiation are also marked. Missing data pertain to b, τ_2 for proton irradiated sample (both fluences), and c, τ_3 of the Cl^{2+} exposed sample at 10^{14} cm^{-2} fluence.

As noted from Eq. (3) the tri-exponential model involves amplitudes and lifetimes a, b, c, τ_1, τ_2, and τ_3 respectively and comparing Eqs. (2) and (3) it is quickly inferred that this type of fit does not provide solution to the rate equation (2) but, only for the purpose of evaluation the magnitudes and type TR-mmWC response changes due to irradiation of Si wafers. However, neglecting the contribution of the band-to-band, and Auger recombination in these irradiated samples (at low pump laser radiation fluence and moderate to low rate of introduction of defects in the lattice due to very low doses of radiation), the solution of the rate Eq. (2) would be represented by the first term on the RHS of the tri-exponential fit Eq. (3) as terms 2 (band-to-band) and 3 (Auger) of Eq. (2) will most likely diminish and could be neglected completely.

Based on this model (Eq. (3)) we compute the differences in time constants $\Delta\tau_1$, $\Delta\tau_2$ and $\Delta\tau_3$ for the 3 exponential terms using the pristine sample data minus the irradiated sample data. Fig. 2(a) shows the log-linear plot of the changes in lifetimes $\Delta\tau_1$, $\Delta\tau_2$ and $\Delta\tau_3$ function of radiation dose in MGy. Crystal defects induced by the gamma and ion beam on Si increase the recombination center densities as a result of which the fitted lifetime is found to slightly differ from that of the pristine Si as shown in Fig. 2(b).

From Fig. 2(a) it is clear that the increase in radiation dose enhances τ_3 and it falls off sharply beyond 0.1 MGy. However, the τ_1 and τ_2 so estimated from data do not abruptly change from those of its parent sample in the wide radiation dose range 1–7 MGy. Fig. 2b shows the same changes $\Delta\tau_i$ but by the exposure type with corresponding dose shown graphically. Measured and SR-NIEL derived radiation doses and SRIM derived defects per ion incident on Si are expected to bear negative correlation with respect to the decay time constants and with respective differences of time constants $\Delta\tau_i$. The τ_{avg} for each sample shows maximum negative correlation with dose ($R = -0.831$) whereas with respect to SRIM defects/ion the correlation coefficient is slightly lower at -0.73. The defects/ion also correlates negatively at -0.77 with $\Delta\tau_2$. Comparing data from Fig. 2b and Table 1 for proton irradiated samples, it is found that even for very low doses of proton bombardment the 4 probe resistivity of the samples enhance to about 10 times and about 4 times for the particle fluence levels of 10^{12} cm^{-2} and 10^{14} cm^{-2} respectively. From Fig. 2b it is evident that τ_1 and τ_2 does not change appreciably over the entire range of irradiation in our analysis and τ_2 duration very slightly increase with a rise in dose however, in general τ_3 is found to remarkably delay with radiation dose.

2.2. Peak response of irradiated sample data

In the previous section we have seen the behavior of photo-induced carrier and its decay patterns as evident from the variation of $\Delta\tau_i$ and the τ_{avg} using the exponentially varying part of the TR-mmWC traces of voltage for each of the irradiated Si wafers. In this section we try to interpret the results of studying the peak power response acquired by the detector for each of those average transients obtained for 4 representative samples each representing the radiation type. TR-mmWC response ratios are plotted as function of laser radiation fluences. From Eq. (1) we note that the TR-mmWC voltage response ratio $\Delta V/V_{dc}$ is related to the change in conductance of the material directly. This peak RF voltage to dc voltage ratio is also related to the corresponding millimeter wave power ratio $\Delta P/P_0$ through the sensitivity factor K. All wafers used in this experiment exhibit millimeter wave transmittance in the range 0.46 to 0.64 at 150 GHz probe frequency with 0.32 mW power. However, we note that irradiation beam energy has some effect on resistivity and the $\Delta V/V_{dc}$ response ratio. Using the detector sensed RF voltages and plotting the TR-mmWC response ratios that the Si wafer when exposed to 2 MeV proton beam with dose of only 5.3 Gray introducing a total vacancy of only 36/ion yields the highest ΔV/DC compared to other exposed samples at a slightly lower beam energy. The same wafer when exposed to 0.75 MeV Cl^{2+} shows lowest response ratio (see Fig. 3). Pristine sample response ratio profile compares well with that of 1.2 MeV γ irradiated sample as seen in Fig. 3.

In fact, the Cl^{2+} irradiated sample response is so low that it had to be multiplied by 1000 in order to include with other samples and to be shown in Fig. 3. From the histogram shown as inset of Fig. 3 it is noted that maximum probability of occurrence of the transmitted peak voltages are in range ~25–50 mV with probabilities 20–40%.

3. Conclusions

Differential absorption-based time-resolved conductivity apparatus (TR-mmWC) operated at 150 GHz with moderate pump laser radiation fluence at wavelength 532 nm has been used to study the effects of Si wafer subjected to 3 different types of radiation possibly introducing crystal lattice damage and vacancies. Average transients of 150 GHz transmitted and reflected RF voltage response of the pristine and irradiated p-type 500 μm thick homogenous Si wafer when excited by the 532 nm pump laser radiation fluence of 10 μJ cm^{-2} with pump-probe spot diameter ratio is ~3.6 are shown. It is noted from these responses that Cl^{2+} ion cause alteration of wafer optical property and as such, its RF transparency is minimal compared to other type of irradiated samples.

Using transient data collected at 150 GHz probe frequency we have attempted to perform an IDA to understand as to how the time constants of the irradiated Si sample decays differ from those obtained for the pure sample. In order to reveal some simple characteristics, these differences are plotted as function of actual and modeled radiation dose and induced vacancies.

We performed an initial decay analysis using the TR-mmWC RF voltage responses by considering a tri-exponential fitting of the decay voltages. We note the differences of the three time constants of irradiated sample RF responses from those of the pristine sample response fits. From this we note the following:

- Increase in radiation dose enhances the third time constant τ_3 and it decays fast beyond 0.1 MGy dose
- Average time constant τ_{avg} shows maximum negative correlation $R = -0.831$ with dose, and $R = -0.73$ with SRIM computed number of defects per ion.
- 4-probe wafer resistivity enhanced to 10x and 4x for 2 MeV proton fluences 10^{12} cm^{-2} and 10^{14} cm^{-2} respectively
- Time constants τ_1 and τ_2 does not change appreciably (from pristine sample values) over the entire range of dose 0.1 to 6 MGy

Peak RF voltages for each of the samples were collected from the pristine and irradiated sample using probe at 150 GHz while sweeping the pump laser radiation fluence between 0.1 μJ cm^{-2} and ~10 μJ cm.$^{-2}$ Using through sample probe DC measurements the peak transmitted voltage ratio $\Delta V_T/V_{dc}$ as function of laser radiation fluence was plotted. This plot helps to point out the following:

- 4-probe wafer resistivity enhanced to 10x and 4x for 2 MeV proton fluences 10^{12} cm^{-2} and 10^{14} cm^{-2} respectively. The reason for enhanced resistivity at a lower particle fluence 10^{12} H^+ cm^{-2} than at 10^{14} H^+ cm^{-2} level is due to the fact that H^+ implantation introduces defects that trap carriers causing already enhanced resistivity at 10^{12} cm^{-2} fluence, however, further increase in particle fluence causes passivation of the traps leading to a lower growth of resistivity.
- 2 MeV H^+ beam exposure enhances the mmw $\Delta V_T/V_{dc}$ response and remains higher than the other responses for each laser radiation fluence point. This is even higher than the pristine Si wafer response
- Cl^{2+} damaged Si wafer exhibits very low ΔV_T /DC compared to other samples exposed to γ, and H^+ radiations, including those of the pristine sample
- Peak transmitted voltages V_T has maximum probability (20–40%) in range 25 to 50 mV

A more systematic study involving silicon irradiated samples at a wider probe frequency range (110–320 GHz) will be beneficial. It will be desirable to study Si wafers having different dopant concentrations and a wide range of resistivity.

CRediT authorship contribution statement

Biswadev Roy: Conceptualization, Data curation, Formal analysis, Methodology, Software, Validation, Visualization, Writing - original draft, Writing - review & editing. **Branko Pivac:** Investigation, Formal analysis, Methodology, Resources, Writing - review & editing. **Branislav Vlahovic:** Funding acquisition, Investigation, Project administration, Resources. **Marvin H. Wu:** Formal analysis, Funding acquisition, Investigation, Project administration, Resources, Supervision, Validation, Writing - review & editing.

Declaration of Competing Interest

The authors declare that they have no known competing financial interests or personal relationships that could have appeared to influence the work reported in this paper.

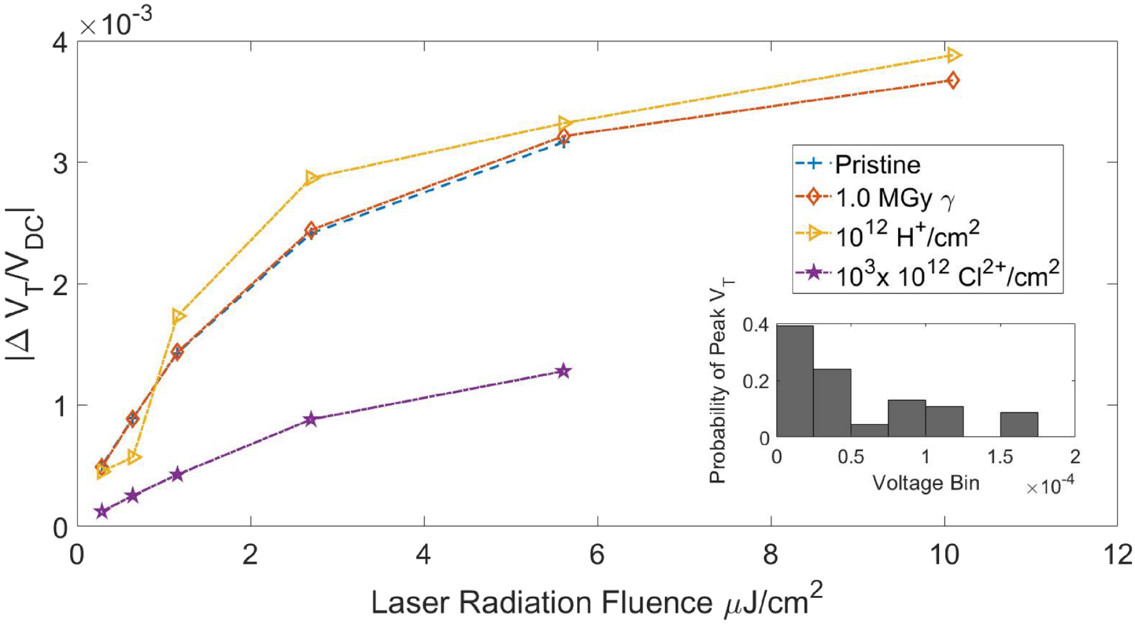

Fig. 3. 150 GHz transmitted (V_{Tpeak}/V_{dc}) vs. laser radiation fluence; inset: probability of peak transmitted voltages through pristine Si, wafer irradiated with 1.0 MGy γ radiation (1.2 MeV), 2 MeV proton with fluence 10^{12} H^+ cm^{-2}, and 1000x the voltage response ratio for the 0.75 MeV irradiated Si sample when exposed to ion fluence 10^{12} Cl^{2+} cm^{-2}.

Acknowledgments

BR acknowledges support received from UNC-General Administration (GA) carbon electronics research opportunities initiative (ROI) and CREST grant from National Science Foundation (HRD-1345219) for carrying out this work. Authors would like to thank Ruder Boskovic Institute, Zagreb, Croatia, for providing the 6 MV Van de Graff facility and Co-60 source for irradiating silicon samples from which this work was made possible. MHW was also partly funded through the NSF partnership for Research and Education in Materials (PREM) program under award No. DMR-1523617.

Appendix A. Supplementary data

Supplementary data to this article can be found online at https://doi.org/10.1016/j.nimb.2020.05.012.

References

[1] N. Kishimoto, H. Amekura, O.A. Plaskin, V.A. Stepanov, Radiation-induced conductivity of doped silicon in response to photon, proton and neutron irradiation, J. Nucl. Mater. 283–287 (2000) 907–911.
[2] J. Krupka, K. Waldemar, P. Kaminski, L. Jensen, Electrical properties of as-grown and proton-irradiated high purity silicon, Nucl. Instrum. Methods Phys. Res. B 380 (2016) 76–83.
[3] N. Kishimoto, H. Amekura, K. Kono, C.G. Lee, Radiation resistance of amorphous silicon in optoelectronic properties under proton bombardment, J. Nucl. Mater. 258–263 (1998) 1908–1913.
[4] J. Warman, P. de Haas Matthjis, H.M. Wentinck, The study of radiation induced conductivity changes in microheterogeneous materials using microwaves, Int. J. Rad. Appl. Instrum., Part C, Radiation Phys. Chem. 34 (4) (1989) 581–586.
[5] H. Amekura, N. Kishimoto, K. Kono, Particle-induced conductivity and photoconductivity of silicon undet 17 MeV proton irradiation, J. Appl. Phys. 84 (9) (1998) 4834–4841.
[6] G. Davies, S. Hayama, L. Murin, R. Krause-Rehberg, V. Bondarenko, A. Sengupta, C. Davia, A. Karpenko, Radiation damage in silicon exposed to high-energy protons, Phys. Rev. B 73 (2006) 165202-1–165202-10.
[7] V. Borjanović, I. Kovačevič, H. Zorc, B. Pivac, Irradiation effects on polycrystalline silicon, Sol. Energy Mater. Sol. Cells 72 (2002) 183–189.
[8] N. Kishimoto, H. Amekura, K. Kono, T. Saito, Radiation-resistant photoconductivity of doped silicon under 17 MeV proton bombardment, J. Nucl. Mater. 233–237 (1996) 1244–1248.
[9] J. Lange, (2008) (2008) Radiation Damage in Proton-Irradiated Epitaxial Silicon Detectors, Ph.D. Thesis, Universität Hamburg, 84 pages.
[10] Z. Li, Radiation damage effects in Si materials and detectors and rad-hard Si detectors for SLHC, PIXEL 2008 International Workshop, Fermilab, U.S.A. 23-26 September, 31 pages, 2008.
[11] A. Picciotto, et al., Boron-proton nuclear-fusion enhancement induced in boron-doped silicon targets by low-contrast pulsed laser, Phys. Rev. X, 4: 031030-1–031030-8, 2014.
[12] J. Kuendig, et al., Thin film silicon solar cells for space applications: Study of proton irradiation and thermal annealing effects on the characteristics of solar cells and individual layers, Sol. Energy Mater. Sol. Cells 79 (4) (2003) 425–438.
[13] A. Ouedraogo, M. Ladifata, Nebon Bado, T.S. Maurice Ky, D.J. Bathiebo, Analysis of the single-crystalline silicon photovoltaic (PV) module performances under low γ-radiation from radioactive source, Silicon (2019), https://doi.org/10.1007/s12633-019-00282-7.
[14] H. Amekura, N. Kishimoto, K. Kono, Radiation-resistant photoconductivity of doped silicon under 17 MeV proton bombardment, J. Nucl. Mater. 233–237 (1996) 1244–1248.
[15] A. Ruzin, G. Casse, M. Glaser, A. Zanet, F. Lemeilleur, S. Watts, Comparison of radiation damage in silicon induced by proton and neutraon irradiation, IEEE Trans. Nucl. Sci. 46 (5) (1999) 1310–1313.
[16] I. Pintilie, G. Lindstroem, A. Junkes, E. Fretwurst, Radiation induced point cluster-related defects with strong impact to damage properties of silicon detectors, Nucl. Instrum. Methods Phys. Res. A: Accelerators, Spectrometers, Detectors and Associated Equipment 611 (2009) 52–68.
[17] B. Roy, C.R. Jones, B. Vlahovic, H.W. Ade, M.H. Wu, A time-resolved millimeter wave conductivity apparatus (TR-mmWC) for charge-dynamical properties of semiconductors, Rev. Sci. Instrum. 89 (10) (2018) 104704.
[18] R.E. Stoller, M.B. Toloczko, G.S. Was, A.G. Certain, S. Dwarknath, F.A. Garner, On the use of SRIM for computing radiation damage exposure, Nucl. Instrum. Methods Phys. Res., B B310 (2013) 75–80.
[19] M.J. Boschini, P.G. Rancoita, M. Tacconi, SR-NIEL Calculator: Screened Relativistic (SR) Treatment for Calculating the Displacement Damage and Nuclear Stopping Powers for Electrons, Protons, Light- and Heavy-Ions in Materials (version 6.0.7). Online available at INFN sez. Milano-Bicocca, Italy 2019 June: http://www.sr-niel.org/, 2014.
[20] J.L. Hesler T.W. Crowe, Responsivity and Noise Measurements of Zero-Bias Schottky Diode Detectors. 18th Intl. Symposium on Space Terahertz Technology, March 2007, Pasadena, 4 pages, 2007.
[21] D.B.M. Klaassen, A unified mobility model for device simulation-II. Temperature dependence of carrier mobility and lifetime, Solid State Electron. 35 (7) (1992) 961–967.
[22] M.J. Kerr, A. Cuevas, General parameterization of Auger recombination in crystalline silicon, J. Appl. Phys. 91 (4) (2002) 2473–2480.